

# Helical Metal Inside a Topological Band Insulator

Ying Ran<sup>1,2</sup>, Yi Zhang<sup>1</sup>, and Ashvin Vishwanath<sup>1,2</sup>

<sup>1</sup>*Department of Physics, University of California, Berkeley, CA 94720*

<sup>2</sup>*Materials Sciences Division, Lawrence Berkeley National Laboratory, Berkeley, CA 94720*

(Dated: Printed October 28, 2008)

Topological defects, such as domain walls and vortices, have long fascinated physicists. A novel twist is added in quantum systems like the B-phase of superfluid helium  $\text{He}_3$ , where vortices are associated with low energy excitations in the cores. Similarly, cosmic strings may be tied to propagating fermion modes. Can analogous phenomena occur in crystalline solids that host a plethora of topological defects? Here we show that indeed dislocation lines are associated with one dimensional fermionic excitations in a ‘topological insulator’, a novel band insulator believed to be realized in the bulk material  $\text{Bi}_{0.9}\text{Sb}_{0.1}$ . In contrast to fermionic excitations in a regular quantum wire, these modes are topologically protected like the helical edge states of the quantum spin-Hall insulator, and not scattered by disorder. Since dislocations are ubiquitous in real materials, these excitations could dominate spin and charge transport in topological insulators. Our results provide a novel route to creating a potentially ideal quantum wire in a bulk solid.

Motivated by applications to spintronics, recent theoretical work on the effect of spin orbit interactions on the band structure of solids predicted the existence of novel ‘topological insulators’ (TIs) in two[1, 2, 3] and three dimensions[4, 5, 6]. In two dimensional TIs (or quantum spin-Hall insulators), in contrast to the gap in the bulk, there are gapless modes at the edge which appear in time reversed pairs with opposite spin and velocity. Transport measurements on  $\text{HgCdTe}$  quantum wells[7, 8] have provided evidence for the existence of these ‘helical’ edge states[1, 9, 10]. In three dimensions, topological insulators are classified as strong ( $\nu_0 = 1$ ) or weak ( $\nu_0 = 0$ ), the former has surface states with an odd number of Dirac points. In addition, 3D TIs are characterized by indices ( $\nu_1, \nu_2, \nu_3$ ) with respect to a basis of reciprocal lattice vectors ( $\vec{G}_1, \vec{G}_2, \vec{G}_3$ ). They define a time reversal invariant momentum (TRIM)  $\vec{M}_\nu = \frac{1}{2}(\nu_1\vec{G}_1 + \nu_2\vec{G}_2 + \nu_3\vec{G}_3)$ . The recent prediction [4] and evidence from angle resolved photoemission experiments [11] for a strong TI phase in the alloy  $\text{Bi}_{0.9}\text{Sb}_{0.1}$ , has led to heightened interest in these systems.

*Dislocations* are line defects of the three dimensional crystalline order, characterized by a vector  $\vec{B}$  (Burgers vector), which is a *lattice vector*. It must remain constant over the entire dislocation. The center of the dislocation is at  $\vec{R}(\sigma)$  where  $\sigma$  parameterizes the line defect. A convenient way to visualize a dislocation is via the Volterra process. One begins with the perfect crystal and chooses a plane  $P$  that terminates along the curve  $\vec{R}(\sigma)$  where the defect is to be produced. The crystal on one side of the plane  $P$  is then displaced by the lattice vector  $\vec{B}$ , and additional atoms are inserted or removed if required. At the end, crystalline order is restored everywhere except near the curve  $\vec{R}(\sigma)$ . A screw dislocation (see Figure 1) is a line defect with its tangent vector  $\vec{t} = d\vec{R}(\sigma)/d\sigma \parallel \vec{B}$ , while an edge dislocation is also a line defect with  $\vec{t} \perp \vec{B}$ . In general, a dislocation varies between these two simple types along its length.

We now state the main result of this paper. Consider a dislocation with Burgers vector  $\vec{B}$  inside a three dimensional topological insulator characterized by ( $\nu_0; \vec{M}_\nu$ ). If

$$\vec{B} \cdot \vec{M}_\nu = \pi \pmod{2\pi} \quad (1)$$

the dislocation induces a pair of one dimensional modes bound to it that traverse the bulk band gap. The modes are related by the Kramers time reversal symmetry transformation and reflect the nontrivial topology of the band structure. We shall refer to this one dimensional state as the ‘helical metal’. While a trivial insulator could also develop one dimensional propagating modes along a dislocation, the precise count obtained here - a single Kramers pair - cannot arise. The topological stability of the helical metal results from time reversal symmetry, which prohibits backscattering between the oppositely propagating modes[2]. From Eqn. 1 we note that some dislocations e.g. with  $\vec{B} \perp \vec{M}_\nu$  do not carry these helical modes. Also, there is the ‘pristine’ strong topological insulator  $\nu_0 = 1, \vec{M}_\nu = 0$ , where none of the dislocations induce helical modes. Experiments indicate that

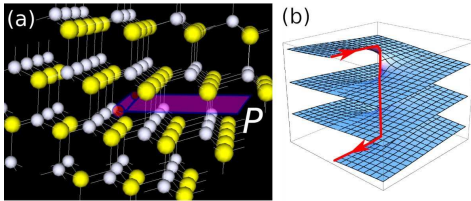


FIG. 1: (color online) [a] Diamond lattice screw dislocation along  $\vec{B} = a(1,1,0)$  direction (shown as a cylinder with red ends). The two diamond sublattices are shown as yellow and white spheres. A cutting plane  $P$  that was used to generate the dislocation is shown, orthogonal to the strength  $t$  bond along  $a/2(1, -1, -1)$ . [b] Screw dislocation in a stacked 2D topological insulator. Unpaired edge modes (one member of the edge mode pair is shown in red) of the top and bottom layer must propagate through the dislocation by continuity.

$\text{Bi}_{0.9}\text{Sb}_{0.1}$  is a strong TI with a nontrivial  $\vec{M}_\nu$ .

**Dislocations in the Diamond Lattice TI** Instead of plunging into a general proof of our results, we first present a numerical calculation of a dislocation in a simple TI model on the diamond lattice[4]:

$$H = t \sum_{\langle ij \rangle} c_{i\sigma}^\dagger c_{j\sigma} + i \frac{8\lambda_{SO}}{(2a)^2} \sum_{\langle\langle ik \rangle\rangle} c_{i\sigma}^\dagger (\vec{d}_{ik}^1 \times \vec{d}_{ik}^2) \cdot \vec{\sigma}_{\sigma\sigma'} c_{k\sigma'}(2)$$

where  $\vec{d}_{ik}^1, \vec{d}_{ik}^2$  are the two nearest neighbor bond vectors leading from site  $i$  to  $k$ ,  $\vec{\sigma}$  are the spin Pauli matrices, and  $2a$  is the cubic cell size. The system is a Dirac metal at this point, and a full gap is opened upon distorting the lattice, by making the nearest neighbor hopping strengths  $t + \delta t$  along one of the directions e.g.  $\frac{a}{2}(1,1,1)$ . If  $\delta t > 0$  ( $\delta t < 0$ ), the system is a strong (weak) topological insulator with  $\nu = 1$  ( $\nu = 0$ ) and  $\vec{M}_\nu = \frac{\pi}{2a}(1,1,1)$ . We now study a screw dislocation and use periodic boundary conditions - which requires us to consider a separated pair of dislocations. Translation symmetry is present along the dislocation axis, and we label states by  $k$ , the crystal momentum in this direction. The precise geometry we use is shown in Figure 1a. If  $\vec{a}_1 = a(0,1,1)$ ,  $\vec{a}_2 = a(1,0,1)$ ,  $\vec{a}_3 = a(1,1,0)$  are the basis vectors, the dislocations are along the  $\vec{a}_3$  axis.

For a pair of unit screw dislocations with  $\vec{B} = a(1,1,0)$ , we find four one dimensional modes, two down moving and two up moving modes, within the bulk gap (Figure 2a). The wavefunctions of these modes are peaked along the two dislocations (Figure 2c) - hence a pair of oppositely propagating modes is present for each dislocation line. The modes are time reversal (Kramers) conjugates of each other. Not all dislocations carry these gapless modes - if we double the Burgers vector of this dislocation (Figure 2b), or consider a different relative orientation when the unequal bond is orthogonal to the Burgers vector (Figure 2d), the one dimensional modes do not appear. The sign of  $\delta t$  is immaterial - both weak and strong topological insulators show this physics.

Note the condition for a gapless line mode to exist on a dislocation *cannot* depend on its orientation, since the modes must propagate through the entire defect. Hence, it can only depend on the Burgers vector  $\vec{B}$ . Therefore, although we have explicitly considered the case of a screw dislocation, the result also holds for an edge or mixed dislocation with the same Burgers vector.

We now present an analytical rationalization for the existence of gapless modes along the dislocation line, in this model of the strong TI. We study the model in a limit that is analytically tractable, but nevertheless adiabatically connected to the parameter regime of interest. Consider the imaginary plane  $P$  (orthogonal to  $(1, -1, -1)$ ), used to construct the dislocation, which ends along the dislocation line. Extend this plane through the entire crystal, weakening all bonds that are cut by it. Now, the crystal is almost disconnected into two disjoint pieces.

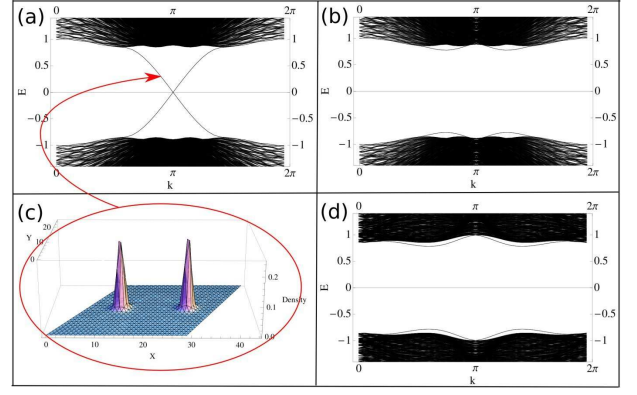


FIG. 2: (color online) Electronic spectrum of the diamond lattice strong TI ( $\vec{M}_\nu = \frac{\pi}{2a}(1,1,1)$ ) in the presence of a pair of screw dislocations. Electronic states are shown as a function of  $k$ , the wavevector along the dislocation. For [a][b][c], the dislocations are oriented along the  $\vec{a}_3 = a(1,1,0)$  axis. [a] Spectrum, when the dislocation Burgers vector  $\vec{B} = \vec{a}_3$  and satisfies  $\vec{B} \cdot \vec{M}_\nu = \pi$ . A pair of counter-propagating modes per dislocation is found, that span the band gap (each midgap level happens to be doubly degenerate). [b] Spectrum when  $\vec{B} = 2\vec{a}_3$  and  $\vec{B} \cdot \vec{M}_\nu = 0 \bmod 2\pi$ . No dislocation modes occur. [c] Probability distribution of a pair of midgap modes shown in the  $\vec{a}_1, \vec{a}_2$  plane that intersects the dislocations. The modes are bound near the dislocations. [d] The dislocations are oriented along  $\vec{B} = a(0,1,-1)$  and  $\vec{B} \cdot \vec{M}_\nu = 0$ . No dislocation modes occur. Calculations were done on a  $36 \times 36 \times 18$  unit cell system with periodic boundary condition along  $\vec{a}_1, \vec{a}_2, \vec{B}$  directions, and dislocations separated by a half system size. The hopping parameters used in Eqn.2 are  $t = 1$ ,  $t + \delta t = 2$ , and  $\lambda_{SO} = 0.125$ .

Gapless states are generated on the two surfaces  $S_+, S_-$ , each with a single Dirac node located at the surface momentum  $\vec{m}_D = \frac{\pi}{2a}(1,1,0)$ . Electronic states in the vicinity of the Dirac point can be expanded as  $\Psi(x_1, x_2) \sim e^{i\vec{m}_D \cdot \vec{x}} \psi(\vec{x})$ , where  $\psi(\vec{x})$  varies slowly over a lattice spacing. The effective Hamiltonian for such states on the two surfaces is  $\pm H_0 = p_1 \sigma_x + p_2 \sigma_y$  [4, 12], where  $p_1, p_2$  are surface momenta measured from the Dirac point, with  $p_1$  along the dislocation line (the  $(1,1,0)$  direction). Thus if  $\mu_z = \pm 1$  represents the two surfaces, the effective Hamiltonian is  $H = H_+(p)\mu_z$ . Now, if we imagine reconnecting the surfaces *without* creating a dislocation, we add a hopping term between the two surfaces:  $H = H_+(p)\mu_z + m\mu_x$ , which leads to fully gapped dispersion, with gap  $2m$ , which can be adiabatically connected to the uniform bulk insulator.

Now consider introducing a screw dislocation, by displacing the surface to one side of the plane  $P$  by the lattice vector  $\vec{B} = a(1,1,0)$ . In our surface coordinate system, the dislocation line is along the  $x_1$  axis, at  $x_2 = 0$ , and the plane  $P$  is at  $x_2 > 0$ . The crucial observation is that when reconnecting the bonds across the plane  $P$ , if the Dirac node is at momentum  $\vec{m}_D$  with  $\vec{m}_D \cdot \vec{B} = \pi$ , then the Dirac particles acquire a *phase*

shift of  $\pi$ . The effective Hamiltonian in the presence of a dislocation is then:  $H_{\text{dis}} = H_+(-i\hbar\nabla)\mu_z + m(x_2)\mu_x$  where the Dirac mass term is:  $m(x_2 < 0) = m$  but  $m(x_2 > 0) = -m$ . Such Dirac Hamiltonians are well known to lead to low energy modes[13] that are protected by index theorems. At  $p_1 = 0$ , a pair of midgap modes are present  $\psi_{\pm}(\vec{x}) = e^{\frac{1}{\pi\nu_2} \int_0^{x_2} dy m(y)} \psi_{0,\pm}$  where  $\psi_{0,\pm}$  are the two solutions of:  $\mu_y \sigma_y \psi_0 = \psi_0$ . For finite  $p_1$  these split to give rise to the left and right moving modes.

More generally, if there are several such surface Dirac modes  $\vec{m}_D^i$ , what is required is that an *odd* number of them acquire a  $\pi$  phase shift on circling the dislocation  $\sum_i \vec{m}_D^i \cdot \vec{B} = \pi(\text{mod } 2\pi)$ . This guarantees the existence of at least a pair of gapless 1D modes on the dislocation. If on the other hand,  $\sum_i \vec{m}_D^i \cdot \vec{B} = 0(\text{mod } 2\pi)$ , there are no protected modes on the dislocation.

**Dislocations in a General TI** Armed with these insights for a specific model, one may discuss the general case of an arbitrary dislocation in a topological band insulator. The condition for the existence of a protected 1D mode is given by equation 1, and derived in the general case in the paragraph below. For the weak TI case, however, a more intuitive derivation of this result is possible. The weak TI is adiabatically connected to a stack of decoupled two dimensional TIs, stacked along the  $\vec{M}_\nu$  direction. The top and bottom surfaces of the stack are fully gapped. Consider creating a screw dislocation in such a stack, by cutting and regluing layers. Cutting a plane results in a pair of edge modes, which are gapped after the planes are glued back together. However, edge modes in the top and bottom layers are left out in this process (see Figure 1b). Since a single pair of such modes cannot begin or end, the helical mode must propagate through the dislocation core to complete the circuit. A similar result holds for three dimensional Chern insulators [14], characterized by a reciprocal lattice vector  $\vec{G}_0$ . There, a dislocation line should have  $\frac{\vec{G}_0 \cdot \vec{B}}{2\pi}$  chiral modes propagating along it.

We now derive the main result equation 1. First, let us briefly review the meaning of the topological insulator invariants ( $\nu_0; \vec{M}_\nu$ ). These are conveniently expressed in terms of quantities  $\delta_{i=(n_1 n_2 n_3)}$  with  $n_i = 0, 1$  defined at the 8 TRIMs of the 3D Brillouin zone(BZ)  $\Gamma_{i=(n_1 n_2 n_3)} = (n_1 \vec{G}_1 + n_2 \vec{G}_2 + n_3 \vec{G}_3)/2$ , which can be computed for a given band structure [4]. The gauge invariant indices are given by:  $(-1)^{\nu_0} = \prod_{n_j=0,1} \delta_{n_1 n_2 n_3}$  and  $(-1)^{\nu_{i=1,2,3}} = \prod_{n_j \neq i=0,1; n_i=1} \delta_{n_1 n_2 n_3}$ . [4] The indices  $\nu_i$  carry information about the surface band structure, in particular, the number of times that the surface bands cross a generic Fermi energy which lies within the bulk gap, along a line in the surface BZ. For example consider the surface spanned by the basis vectors  $\vec{a}_1, \vec{a}_2$  normal to  $\vec{G}_3$ . The parity (even vs odd) of the number of such band crossings  $N_{\text{cross}}$ , when connecting two surface

TRIMs  $\vec{m}_1, \vec{m}_2$  is a topologically protected quantity [4]:

$$(-1)^{N_{\text{cross}}} = \delta_{\vec{m}_1} \delta_{\vec{m}_2} \delta_{\vec{m}_1 + \frac{\vec{G}_3}{2}} \delta_{\vec{m}_2 + \frac{\vec{G}_3}{2}}. \quad (3)$$

Thus  $\nu_1 = N_{\text{cross}}(\text{mod } 2)$  between  $\vec{m}_1 = \frac{\vec{G}_1}{2}$  and  $\vec{m}_2 = \frac{\vec{G}_1 + \vec{G}_2}{2}$  on this surface.

Without loss of generality, consider now creating a screw dislocation in a TI with Burgers vector  $\vec{B} = \vec{a}_1$ . This is created using the Volterra procedure by a cutting  $\vec{a}_1 - \vec{a}_2$  surface containing the dislocation. Atoms on one side of the surface are displaced by  $\vec{B}$  and reconnected. The crucial step in our analytical derivation of the helical modes was whether there are even or odd number of surface Dirac nodes that acquire a  $\pi$  phase shift on creating the dislocation. Although in general, the surface band structure may be quite complicated, for the purpose of deriving robust topological properties one may adiabatically deform the crystal structure (during which the bulk gap remains open, *and* the Bravais lattice structure stays fixed) so that the surface modes are always Dirac nodes that cross the band gap, centered at the surface TRIMs. Then, there are two surface TRIMs  $\vec{m} = \{\frac{\vec{G}_1}{2}, \frac{\vec{G}_1 + \vec{G}_2}{2}\}$  for which  $\vec{B} \cdot \vec{m} = \pi(\text{mod } 2\pi)$ , i.e. acquire a  $\pi$  phase shift on creating the dislocation. If the number of surface Dirac nodes present in total at these two TRIMs  $N_{\text{Dirac}}$  is odd, then the dislocation will host a protected helical mode. Clearly, the parity of  $N_{\text{Dirac}}$  is the same as the number of band crossings between the two surface TRIMs given by Equation 3. Thus, the condition for the helical modes is  $\nu_1 = 1$  or  $\vec{M}_\nu \cdot \vec{B} = \pi(\text{mod } 2\pi)$ .

In general, the Burgers vector is a multiple of the primitive lattice vector. If it is an odd multiple, the derivation above is unaffected. If it is an even multiple, there are no dislocation modes since the phase shifts are always trivial. Hence we arrive at 1, for the existence of protected helical modes along the dislocation.

**Effect of Disorder** It is sometimes stated that in the presence of disorder, only the  $\nu_0$  index is robust, while the  $\vec{M}_\nu$  index is irrelevant. Hence weak TIs are believed to be unstable in the presence of disorder [4]. Since our results are controlled precisely by the  $\vec{M}_\nu$  index, they shed light on when they retain meaning. If the disorder is so strong that the dislocations are no longer well defined, then the only remaining distinction is the  $\nu_0$  index. Similarly, an insulator with  $\vec{M}_\nu = 0$  can be converted to one with  $\vec{M}_\nu \neq 0$ , by introducing a potential modulation with period  $\vec{M}_\nu$ . Elementary dislocations that carry helical modes will then cost infinite energy per unit length. However, for a sufficiently weak disorder potential, the dislocations are expected to remain well defined, in which case the distinction captured by  $\vec{M}_\nu$  is physically relevant. Certainly, in real crystals which are inevitably disordered, dislocations are well defined objects, and hence the physics discussed in this paper should apply.

**Experimental Consequences** In real solids, dislocations are always present and the predicted helical modes

should have important experimental consequences. Scanning tunneling microscopy (STM) of a topological insulator surface where dislocations terminate, is particularly well suited to verify these predictions. Since the precise atomic arrangement is visualized by STM, the nature of the dislocations involved can be characterized. At the same time, the finite density of states associated with the one dimensional modes will lead to an enhanced tunneling density of states near the dislocation core. This will be particularly striking if one tunes to an energy where the surface modes contribute minimally (eg. at the Dirac node). Such experiments are immediately feasible on the putative topological insulator  $\text{Bi}_{0.9}\text{Sn}_{0.1}$  with A7 structure. Since the band structure of that material is complex and still debated [15], we demonstrate qualitatively what is expected, in the simpler diamond lattice strong TI model 2. Moreover, since the crystal symmetry in the two cases share several features - such as a three fold axis parallel to the  $\vec{M}_\nu$  vector, some predictions for the diamond lattice model may be directly relevant to the A7 structure. First consider the surface orthogonal to the strong bond (1,1,1) direction. We choose this surface to cut three strength  $t$  bonds (rather than a single strong bond) in order to obtain a surface band structure similar in some respects to the (111) surface of  $\text{Bi}_{0.9}\text{Sn}_{0.1}$ . We call this the (111)' surface. This surface has a single Dirac node centered at the  $\Gamma$  point. We consider a pair of separated screw dislocations with  $\vec{B} = a(1,1,0)$ , which carry 1D helical modes, that terminate on the surface. STM measures the local density of states (LDOS) at a given energy and surface location  $\rho(\vec{r}, E) = \sum_\alpha |\psi_\alpha(\vec{r})|^2 \delta(E - E_\alpha)$ , where the  $\alpha$  sum runs over all eigenstates. The dislocations appear as peaks in the LDOS as shown in Figure 3a, due to these helical modes. Note, the ledge connecting the two screw dislocations on the surface also shows an enhanced DOS.

More striking evidence for the relation 1 appears when we consider the edge dislocations on the  $(\bar{1}\bar{1}1)$  surface. If the Burgers vector of the dislocation is  $\vec{B} = a(1, 0, 1)$  the one dimensional modes are present and visible in the LDOS (Figure 3b), but if  $\vec{B} = a(1, -1, 0)$  then they are absent (Figure 3c). Here, there is no physical line connecting the two defects.

Since elastic scattering by nonmagnetic impurities cannot scatter electrons between the counter-propagating helical modes of the dislocation, they behave as ideal quantum wires which may be relevant for spin and charge transport applications at low temperatures when inelastic processes are frozen out. The challenge will be to separate this conduction mechanism from protected surface mode conduction, which is also present. In conduction across the short direction of anisotropic samples (eg. disc shaped), dislocation induced direct conduction paths should dominate over surface conduction. If dislocations can be induced in a controlled fashion during the growth process, then the direction dependent condition for the

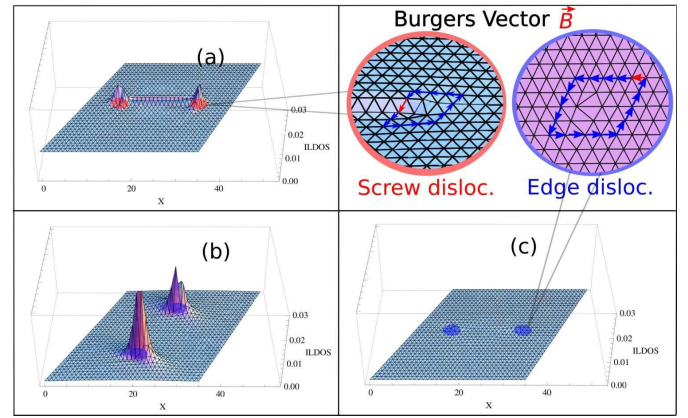


FIG. 3: (color online) Surface LDOS as measured by STM, for various dislocation configurations, in the diamond lattice strong TI with parameters as in Fig.2. In all cases dislocation pairs are separated by a half system size, and are directed along  $\vec{a}_3$ . Topography of the integrated LDOS in the energy window  $[-0.1, 0.1]$  is shown, with insets displaying energy dependent LDOS at special points on the surface. [a] The (111)' surface intersecting a pair of screw dislocations with  $\vec{B} = a(1,1,0)$ . These carry 1D modes which give rise to a peak in the integrated LDOS. In [b] and [c], edge dislocations on the  $(\bar{1}\bar{1}1)$  surface. In [b], the dislocation satisfies  $\vec{B} \cdot \vec{M}_\nu = \pi$ , and has 1D modes visible in the LDOS while in [c] the dislocation has  $\vec{B} \cdot \vec{M}_\nu = 0$ , hence no 1D line mode and no enhanced LDOS. In [a][b][c] only the top layer of atoms is shown, and calculations are done on  $36 \times 36 \times 18$  unit cell system, with periodic boundary conditions in the  $\vec{a}_1, \vec{a}_2$  directions.

existence of helical modes, and dislocation density dependence of conductivity can be used to isolate this contribution. Another possibility is to introduce magnetic impurities on the surface of the insulator, which could potentially localize surface modes but have little impact on dislocation helical modes deep in the bulk. A rough estimate of the excess electric conductivity induced by dislocation modes for a dislocation density  $n_d \sim 10^{12} \text{m}^{-2}$  and a low temperature scattering length  $l \sim 1 \mu\text{m}$  along the dislocation [8] yields  $\rho = \frac{h}{2e^2} \frac{1}{n_d l} \sim 10 m\Omega\text{m}$ , which should be experimentally accessible.

Funding from NSF DMR-0645691 is acknowledged.

- 
- [1] C. L. Kane and E. J. Mele, Phys. Rev. Lett. **95**, 226801 (2005).
  - [2] C. L. Kane and E. J. Mele, Phys. Rev. Lett. **95**, 146802 (2005).
  - [3] B. A. Bernevig and S.-C. Zhang, Phys. Rev. Lett. **96**, 106802 (2006).
  - [4] L. Fu, C. L. Kane, and E. J. Mele, Phys. Rev. Lett. **98**, 106803 (2007).
  - [5] J. E. Moore and L. Balents, Phys. Rev. B **75**, 121306 (2007).
  - [6] R. Roy (2006), URL <http://www.citebase.org/abstract?id=oai:ar>

- [7] B. A. Bernevig, T. L. Hughes, and S.-C. Zhang, *Science* **314**, 1757 (2006).
- [8] M. Koenig, S. Wiedmann, C. Bruene, A. Roth, H. Buhmann, L. W. Molenkamp, X.-L. Qi, and S.-C. Zhang, *Science* **318**, 766 (2007).
- [9] C. Wu, B. A. Bernevig, and S.-C. Zhang, *Phys. Rev. Lett.* **96**, 106401 (2006).
- [10] C. Xu and J. E. Moore, *Phys. Rev. B* **73**, 045322 (2006).
- [11] D. Hsieh, D. Qian, L. Wray, Y. Xia, Y. S. Hor, R. J. Cava, and M. Z. Hasan, *Nature* **452**, 970 (2008).
- [12] L. Fu and C. L. Kane, *Phys. Rev. Lett.* **100**, 096407 (2008).
- [13] C. Callan and J. Harvey, *Nuclear Physics B* **250**, 427 (1985).
- [14] M. Kohmoto, B. I. Halperin, and Y.-S. Wu, *Phys. Rev. B* **45**, 13488 (1992).
- [15] J. C. Y. Teo, L. Fu, and C. L. Kane, *Phys. Rev. B* **78**, 045426 (2008).